Cluster Compounds

DOI: 10.1002/ange.201103127

Lanthanide Antimony Oxohalides: From Discrete Nanoclusters to Inorganic–Organic Hybrid Chains and Layers**

*Bing Hu, Mei-Ling Feng, Jian-Rong Li, Qi-Pu Lin, and Xiao-Ying Huang**

High-nuclearity cluster compounds are of continuing interest not only because of their diverse molecular structures but also for their intriguing physical and chemical properties.[1] For example, lanthanide cluster compounds often exhibit unique magnetic and luminescent properties.[2] Recently, high-nuclearity clusters as secondary building units (SBUs) acting as nodes have been introduced to construct diversiform inorganic–organic hybrid structures with organic ligands with different geometry as linkers.[3] Clusters as rigid SBUs, especially expanded to nanometer sizes, are better than single metal ion nodes at maintaining specific geometries and imparting physical properties to hybrids through the assembly process.[4]

Low-dimensional metal oxohalides are attractive because of their pleasing structures and specific properties, such as magnetic frustration and anisotropic conductivity.[5] Studies indicate that the incorporation of lone-pair cations such as Pb^{II}, As^{III}, Sb^{III}, Bi^{III}, and Te^{IV} into oxohalides, could increase the possibility of obtaining low-dimensional structures in which both halide ion and lone pair act as "structural scissors". This synthesis concept was realized in the search for new transition-metal oxohalides with reduced dimensionality.[5c–o] Herein, we demonstrate that this strategy could also be an effective way to construct novel low-dimensional rare-earth oxohalides. By integrating praseodymium ion (Pr^{3+}) with the lone-pair Sb^{3+} cation, the first molecular lanthanide antimony oxohalide, namely, (2-MepyH)$_5$[$Pr_4Sb_{12}O_{18}Cl_{17}$] (**1**) (2-Mepy = 2-methylpyridine), which features a nanocluster of $[Pr_4Sb_{12}O_{18}Cl_{17}]^{5-}$, was obtained. More significantly, utilizing the inorganic nanocluster as node and angular or linear carboxylic ligands as linkers, two hybrid compounds with one-dimensional (1D) chain and two-dimensional (2D) layer structure were constructed, namely, (2-MepyH)$_4$[$Pr_4Sb_{12}O_{18}Cl_{14}$(1,3-bdc)] (**2**) (1,3-bdcH$_2$ = 1,3-benzenedicarboxylic acid) and (2-MepyH)$_3$[$Pr_4Sb_{12}O_{18}Cl_{11}$(1,4-bdc)$_2$]·4.5 H_2O (**3**) (1,4-bdcH$_2$ = 1,4-benzenedicarboxylic acid).

Compound **1** was synthesized by solvothermal reaction of $Pr(AcO)_3 \cdot 3H_2O$ (AcO = acetate) and $SbCl_3$, in a mixture of H_2O and 2-Mepy at 160 °C for 3 days. Single-crystal X-ray diffraction reveals that **1** belongs to the noncentrosymmetric space group *R*3*m* with the asymmetric unit containing one-sixth of the formula unit. Compound **1** consists of a nearly perfect T_d-symmetric anionic nanocluster of $[Pr_4Sb_{12}O_{18}Cl_{17}]^{5-}$ and five monoprotonated 2-methylpyridine (2-MepyH$^+$) molecules as counterions. As seen in Figure 1,

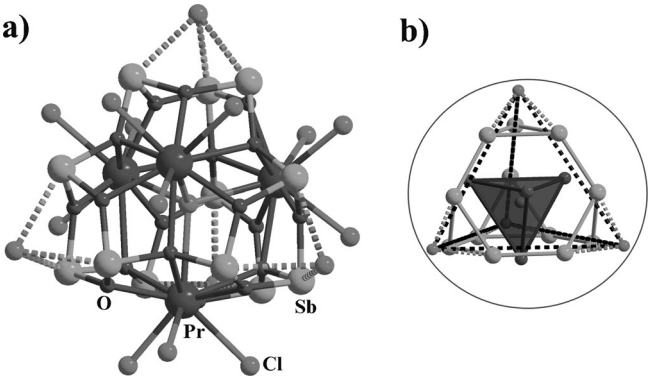

Figure 1. a) The anionic nanocluster $[Pr_4Sb_{12}O_{18}Cl_{17}]^{5-}$ with nearly perfect T_d symmetry in **1**. b) The inverted {Pr_4} tetrahedron is encapsulated in the large truncated tetrahedral {Sb_{12}} cage.

the discrete noncentrosymmetric cluster contains four Pr^{3+} cations, twelve Sb^{3+} cations, one μ_4-Cl^- ion, six μ_4-O ions, twelve μ_3-O ions, twelve terminal Cl^- ions, and four additional Cl^- ions forming secondary bonds with Sb^{3+} only. The four Pr^{3+} cations are arranged in almost perfect tetrahedral symmetry (Pr–Pr = 4.830(2)–4.838(2) Å) with the μ_4-Cl^- ion lying at the centre (Pr–μ_4-Cl = 2.950(3)–2.9644(12) Å) of the tetrahedron. Each of the decacoordinated Pr^{3+} ions connects one μ_4-Cl, three μ_3-O, three μ_4-O, and three terminal Cl^- ions (Pr–Cl = 2.862(3)–2.932(2) Å) to complete a monotruncated hexagonal bipyramid configuration. Each of the μ_4-O ligands is located near the middle of each edge of the {Pr_4} tetrahedron connecting two Pr^{3+} and two Sb^{3+} ions, whereas each of the μ_3-O group is located above the face of the {Pr_4} tetrahedron linking one Pr^{3+} and two Sb^{3+} ions. As a consequence, three μ_3-O groups interlink three Sb^{3+} ions to constitute a {Sb_3O_3} ring capping each face of the Pr_4 tetrahedron like a crown. Therefore, the whole cluster can be denoted as a small, inverted {Pr_4} tetrahedron encapsulated within a larger truncated tetrahedral cage made up of twelve Sb^{3+} ions, in which each three Sb^{3+} ions hold the truncated position (Figure 1 b). In the cluster, each of the Sb^{3+}

[*] Dr. B. Hu, Dr. M.-L. Feng, Dr. J.-R. Li, Dr. Q.-P. Lin, Prof. X.-Y. Huang
State Key Laboratory of Structural Chemistry, Fujian Institute of Research on the Structure of Matter, Chinese Academy of Sciences, Fuzhou, Fujian 350002 (P. R. China)
E-mail: xyhuang@fjirsm.ac.cn

[**] This work was supported by the Knowledge Innovation Program of the Chinese Academy of Sciences (KJCX2-YW-H21), the NNSF of China (Grants 20771102, 20873149, 20803081, and 21001104), and the NSF of Fujian Province (Grants 2008J0174 and 2010J01056).

Supporting information for this article is available on the WWW under http://dx.doi.org/10.1002/anie.201103127.

cations exhibits trigonal-pyramidal geometry and coordinates to three oxygen atoms (Sb–O = 1.978(3)–2.000(3) Å) and further interacts with a Cl^- ion (Sb–Cl = 2.9560(1)–3.0670(1) Å) to form a potential pseudo-trigonal-bipyramidal environment of $[SbO_3ClE]$ (E = lone pair). Each of the four additional Cl^- ions lying on the crystallographic threefold rotational axis is shared by three Sb cations of one "crown" and occupies the vertex of a larger $\{Cl_4\}$ tetrahedron (Figure 1b). As a result, the $[Pr_4Sb_{12}O_{18}Cl_{17}E_{12}]^{5-}$ anion cluster involves 12 lone pairs and 16 Cl^- ions in total on its surface. The distances from the vertex Cl^- to the central μ_4-Cl^- ion are in the range 5.855(7)–5.949(14) Å, resulting in a diameter of the whole cluster of around 15.5 Å assuming a van der Waals radius of Cl^- ion of 1.8 Å. The 2-MepyH$^+$ counterions sit in the intervening space among anionic clusters to balance the charge.

In this type of oxohalide, Pr^{3+} is more "halophilic" than the lone-pair cation Sb^{3+}, which is more "oxophilic". As a result, Pr^{3+} coordinates with both O^{2-} and Cl^-, whereas Sb^{3+} associates exclusively with O^{2-}, having only secondary bonding interactions with the crown capping Cl^- ions. The lone pair and the Cl^- anion help to reduce the dimensionality of the whole structure, illustrating a good example of a "structure scissor" strategy in constructing low-dimensional structures. Although a series of low-dimensional lone-pair metal oxohalides have been obtained,[5c–q] compound **1** represents the first heterometallic cluster-like oxohalide by integrating Pr^{3+} with lone-pair Sb^{3+} cation.

The $[Pr_4Sb_{12}O_{18}Cl_{17}]^{5-}$ cluster contains sixteen Cl^- anions on the surface, which offers the possibility for constructing inorganic–organic hybrid structures by substituting the Cl^- ions of the cluster with organic ligands. Fortunately, using two types of bridging carboxylic ligands 1,3-bdc and 1,4-bdc, 1D compound **2** and 2D compound **3** were obtained.

Single-crystal X-ray diffraction analysis reveals that compound **2** belongs to the monoclinic space group $P2_1/c$. The asymmetric unit of **2** contains one $[Pr_4Sb_{12}O_{18}Cl_{14}]^{2-}$ cluster, one 1,3-bdc ligand, as well as three entire and two half 2-MepyH$^+$ cations. In **2**, the structure of the cluster is similar to that in **1**, except that three of the terminal Cl^- ions from two Pr^{3+} centers are substituted by two carboxylate groups (Figure 2. The 1,3-bdc ligand is tridentate; it chelates with one Pr^{3+} cation from one cluster and also bridges another Pr^{3+} cation from another cluster (Figure 3a). Thus the interconnection of the nanoclusters by 1,3-bdc ligands results in a zigzag chain along the *c* axis (Figure 2). The 2-MepyH$^+$ counterions are located among the anion chains and form N–H···Cl and N–H···O hydrogen-bonding interactions with the anionic clusters.

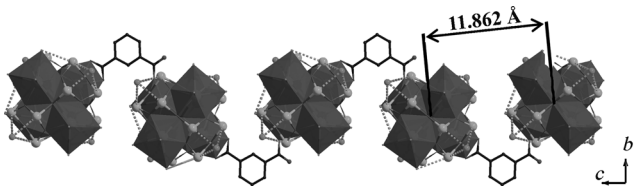

Figure 2. Polyhedral view of the zigzag chain running along the *c* axis in compound **2**.

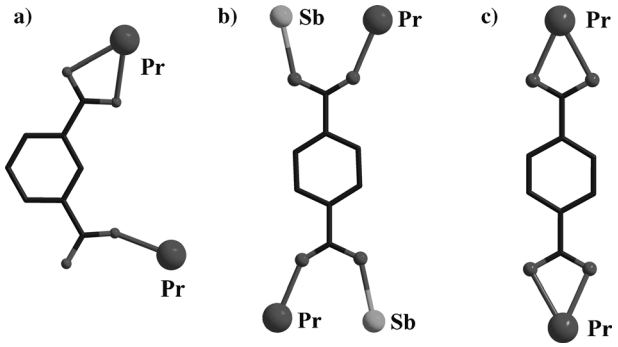

Figure 3. Coordination modes of a) 1,3-bdc in **2**, and b,c) 1,4-bdc in **3**.

Compound **3** belongs to the monoclinic space group *C2/c*, and exhibits 2D wavelike layer structure. The asymmetric unit of **3** contains half of the $[Pr_4Sb_{12}O_{18}Cl_{11}]^+$ cluster, two halves of an 1,4-bdc ligand, one and a half 2-MepyH$^+$ cations, two and one fourth lattice water molecules. The $[Pr_4Sb_{12}O_{24}Cl_{11}]^{5-}$ cluster of **3** could be viewed as a derivative of the $[Pr_4Sb_{12}O_{18}Cl_{17}]^{5-}$ cluster in **1** as four terminal Cl^- ions from two Pr^{3+} ions are substituted by four O atoms from two chelating carboxylate groups, and two terminal Cl^- ions from another two Pr^{3+} ions are substituted by two O atoms from two bridging carboxylate groups. Thus, the 1,4-bdc ligands interconnect the metal ions from two neighboring clusters in two different fashions (Figure 3b,c). As a result, each $[Pr_4Sb_{12}O_{18}Cl_{11}]^+$ cluster links to four adjacent clusters through four 1,4-bdc ligands forming a 2D wavelike layer along the *ac* plane (Figure 4). The 2D layers are stacked in parallel along the *b* axis with the wave crest embedded in the trough of the neighboring wave. The 2-MepyH$^+$ cations are located between the adjacent anionic layers with hydrogen-bonding interactions of N–H···Cl and N–H···O, and the lattice water molecules connect the neighboring layers into three-

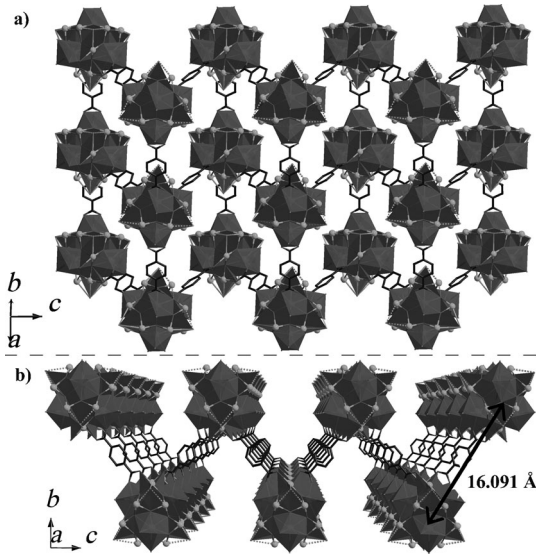

Figure 4. Polyhedral view of the wavelike sheet along the [110] direction (a) and *a* axis (b) in compound **3**.

dimensional supramolecular structure through O–H···Cl and O–H···O hydrogen bonds.

The distances between the two central Cl atoms of the nearest neighboring clusters are 12.081 Å in the structure of **1** and 11.862 Å in the common chain in **2**, whereas it is 16.091 Å in the common sheet in **3**, indicating that the angular ligand 1,3-bdc draws the neighboring clusters closer while the linear 1,4-bdc pushes them away from each other. Meanwhile, the shortest distance between central Cl^- from neighboring layers in **3** is 11.860 Å, which is slightly shorter than the separation of 12.081 Å between the discrete clusters in **1**, which probably is due to the close packing of neighboring layers in **3** (Figure S5 in the Supporting Information).

The thermal stabilities of the three cluster-based compounds were characterized (Figure S7) by thermogravimetric analyses. As indicated by powder X-ray diffraction, **1** and **2** are stable up to 260 °C, and the crystal structure of **3** can be maintained at 320 °C (Figures S9–S11). The thermal decomposition products of **1**, **2**, and **3** were all identified to contain Sb_6O_{13} (Figure S12) and unidentified powder. The optical absorption spectra of **1**, **2**, and **3** were measured by diffuse-reflectance experiments, indicating the absorption edges of 4.1, 4.0, and 3.6 eV, respectively (Figure S13).

As compound **1** crystallizes in the noncentrosymmetric space group *R*3*m*, second harmonic generation (SHG) measurements on crystalline sample of **1** using 1064 nm radiation revealed that **1** exhibited a SHG response about 0.31 times that of potassium dihydrogen phosphate (KDP). Ferroelectric measurements on a single crystal of **1** presented a banana-shaped electric hysteresis loop, showing a remanent polarization ($P_r \approx 0.2\ \mu C\,cm^{-2}$) (Figure S14). As the cluster as a whole has no polarization, it is unlikely that the dipole moments associated with the asymmetric SbO_3 polyhedra are reversible.[6] The electronic polarization of the compound may derive from the noncentrosymmetric arrangement of the clusters in the structure.

In summary, we have prepared the first lanthanide antimony oxohalide nanometer-sized cluster with nearly perfected T_d symmetry using a "structure scissor" strategy, in which lone pairs and halide ions play important roles in constructing the discrete structure. Furthermore, by substituting partially the Cl^- supporting ligands with dicarboxylate ligands with angular or linear linking geometry, hybrids with 1D chainlike and 2D wavelike structures were realized. Thus, it is hoped to design more diversiform inorganic–organic hybrid low-dimensional structures based on the high-nuclearity cluster SBUs by introducing diverse ligands.

Experimental Section

Syntheses of **1**, **2**, and **3**: A mixture of $Pr(AcO)_3{\cdot}3H_2O$ (1.0 mmol, 0.408 g) and $SbCl_3$ (3.0 mmol, 0.682 g) in mixture of 2-Mepy (5.0 mL) and H_2O (1.5 mL) was sealed in a 28 mL teflon-lined stainless-steel autoclave at 160 °C for 4 days (caution: $SbCl_3$ is corrosive!). Green blocklike crystals of **1** (manually selected, yield: 0.536 g, 63 % based on Pr) and unknown white powder were obtained upon cooling to room temperature. Elemental analysis (%): calcd for $C_{30}H_{40}Cl_{17}N_5O_{18}Pr_4Sb_{12}$ (**1**): C 10.64, H 1.90, N 2.07; found: C 10.82, H 1.55, N 2.08.

A similar reaction was carried out by adding 1,3-bdcH_2 (0.25 mmol, 0.042 g) and NaOH (0.5 mmol, 0.020 g). The green platelike crystals of **2** (manually selected, yield: 0.469 g, 56 % based on Pr) and unknown white powder were obtained by filtration and air-dried. Elemental analysis (%): calcd for $C_{32}H_{36}Cl_{14}N_4O_{22}Pr_4Sb_{12}$ (**2**): C 11.47, H 1.08, N 1.67, O 10.51; found: C 11.35, H 0.99, N 1.63, O 11.17.

A similar reaction was carried out by adding 1,4-bdcH_2 (0.5 mmol, 0.084 g) and NaOH (1.0 mmol, 0.040 g). The green prismatic crystals of **3** (manually selected, yield: 0.407 g, 48 % based on Pr) and unknown white powder were obtained by filtration and air-dried. Elemental analysis (%): calcd for $C_{34}H_{41}Cl_{11}N_3O_{30.5}Pr_4Sb_{12}$ (**3**): C 11.89, H 1.22, N 1.24, O 14.38; found: C 11.68, H 1.16, N 1.22, O 14.02.

Energy-dispersive X-ray spectroscopy, powder X-ray Diffraction, thermogravimetric analysis, diffuse-reflectance spectroscopy, and magnetic measurement results for **1**, **2**, and **3**, and SHG and ferroelectric measurement results of **1** are shown in the Supporting Information.

Crystal data for **1**: $C_{30}H_{40}Cl_{17}N_5O_{19}Pr_4Sb_{12}$, $M = 3402.11$, hexagonal, *R3m*, $a = 18.2342(5)$, $c = 17.7781(9)$ Å, $V = 5119.0(3)$ Å^3, $Z = 3$. $\rho_{calcd} = 3.295\ g\,cm^{-3}$, $F(000) = 4608$, $\mu = 8.182\ mm^{-1}$, $2.33 < \theta < 27.48°$, $T = 293(2)$ K, 14525 reflections measured, 2851 unique reflections ($R_{int} = 0.0408$), 2754 observed reflections [$I > 2\sigma(I)$] with $R_1(wR_2) = 0.0242$ (0.0610), $R_1(wR_2) = 0.0306$ (0.0793) (all data). GOF = 1.008. Crystal dimensions: $0.22 \times 0.22 \times 0.20\ mm^3$.

Crystal data for **2**: $C_{32}H_{36}Cl_{14}N_4O_{22}Pr_4Sb_{12}$, $M = 3349.73$, monoclinic, $P2_1/c$, $a = 12.2034(4)$, $b = 25.0516(6)$, $c = 23.5552(5)$ Å, $\beta = 101.365(2)°$, $V = 7060.0(3)$ Å^3, $Z = 4$. $\rho_{calcd} = 3.151\ g\,cm^{-3}$, $F(000) = 6072$, $\mu = 7.803\ mm^{-1}$, $2.34 < \theta < 28.90°$, $T = 293(2)$ K, 25359 reflections measured, 14811 unique reflections ($R_{int} = 0.0586$), 11292 observed reflections [$I > 2\sigma(I)$] with $R_1(wR_2) = 0.0444$ (0.1031), $R_1(wR_2) = 0.0609$ (0.1075) (all data). GOF = 1.078. Crystal dimensions: $0.42 \times 0.35 \times 0.22\ mm^3$.

Crystal data for **3**: $C_{34}H_{41}Cl_{11}N_3O_{30.5}Pr_4Sb_{12}$, $M = 3394.29$, monoclinic, *C2/c*, $a = 16.0446(4)$, $b = 26.2243(8)$, $c = 17.4800(4)$ Å, $\beta = 91.293(2)°$, $V = 7353.0(3)$ Å^3, $Z = 4$. $\rho_{calcd} = 3.066\ g\,cm^{-3}$, $F(000) = 6180$, $\mu = 7.396\ mm^{-1}$, $2.33 < \theta \le 27.48°$, $T = 293(2)$ K, 15168 reflections measured, 7340 unique reflections ($R_{int} = 0.0331$), 6427 observed reflections [$I > 2\sigma(I)$] with $R_1(wR_2) = 0.0512$ (0.1384), $R_1(wR_2) = 0.0595$ (0.1450) (all data). GOF = 1.053. Crystal dimensions: $0.26 \times 0.18 \times 0.08\ mm^3$.

The intensity data were collected on a Rigaku SCXmini CCD diffractometer for **1** and on an Oxford Xcalibur Eos CCD diffractometer for **2** and **3** at room temperature with graphite-monochromated $Mo_{K\alpha}$ radiation ($\lambda = 0.71073$ Å). The structures were solved by direct methods and refined by full-matrix least-squares analysis on F^2 using the SHELXL97 program package. CCDC 822912 (**1**), 822913 (**2**), and 822914 (**3**) contain the supplementary crystallographic data for this paper. These data can be obtained free of charge from The Cambridge Crystallographic Data Centre via www.ccdc.cam.ac.uk/data_request/cif.

Received: May 6, 2011
Published online: July 14, 2011

Keywords: cluster compounds · lone pairs · organic–inorganic hybrid composites · oxohalides · solid-state structures

[1] a) G. E. Kostakis, A. M. Ako, A. K. Powell, *Chem. Soc. Rev.* **2010**, *39*, 2238–2271; b) T. K. M. Lee, N. Y. Zhu, V. W. W. Yam, *J. Am. Chem. Soc.* **2010**, *132*, 17646–17648.

[2] a) R. Sessoli, A. K. Powell, *Coord. Chem. Rev.* **2009**, *253*, 2328–2341; b) P. H. Lin, T. J. Burchell, L. Ungur, L. F. Chibotaru, W. Wernsdorfer, M. Murugesu, *Angew. Chem.* **2009**, *121*, 9653–9656; *Angew. Chem. Int. Ed.* **2009**, *48*, 9489–9492; c) J. Rocha, L. D.

Carlos, F. A. A. Paz, D. Ananias, *Chem. Soc. Rev.* **2011**, *40*, 926 – 940.

[3] a) S. T. Zheng, J. Zhang, G. Y. Yang, *Angew. Chem.* **2008**, *120*, 3973 – 3977; *Angew. Chem. Int. Ed.* **2008**, *47*, 3909 – 3913; b) H. C. Zhou, J. R. Li, A. A. Yakovenko, W. G. Lu, D. J. Timmons, W. J. Zhuang, D. Q. Yuan, *J. Am. Chem. Soc.* **2010**, *132*, 17599 – 17610.

[4] a) Y. G. Huang, F. L. Jiang, M. C. Hong, *Coord. Chem. Rev.* **2009**, *253*, 2814 – 2834; b) U. Schubert, *Chem. Soc. Rev.* **2011**, *40*, 575 – 582.

[5] a) N. R. M. Crawford, J. R. Long, *Inorg. Chem.* **2001**, *40*, 3456 – 3462; b) N. G. Naumov, S. Cordier, C. Perrin, *Angew. Chem.* **2002**, *114*, 3128 – 3130; *Angew. Chem. Int. Ed.* **2002**, *41*, 3002 – 3004; c) M. Johnsson, K. W. Tornroos, P. Lemmens, P. Millet, *Chem. Mater.* **2003**, *15*, 68 – 73; d) P. Lemmens, K. Y. Choi, G. Guntherodt, M. Johnsson, P. Millet, F. Mila, R. Valenti, C. Gros, W. Brenig, *Phys. B* **2003**, *329*, 1049 – 1050; e) R. Becker, M. Johnsson, R. K. Kremer, P. Lemmens, *J. Solid State Chem.* **2005**, *178*, 2024 – 2029; f) R. Becker, H. Berger, M. Johnsson, M. Prester, Z. Marohnic, M. Miljak, M. Herak, *J. Solid State Chem.* **2006**, *179*, 836 – 842; g) R. Becker, M. Johnsson, R. K. Kremer, H. H. Klauss, P. Lemmens, *J. Am. Chem. Soc.* **2006**, *128*, 15469 – 15475; h) R. Takagi, M. Johnsson, V. Gnezdilov, R. K. Kremer, W. Brenig, P. Lemmens, *Phys. Rev. B* **2006**, *74*, 014413; i) Z. Mayerová, M. Johnsson, S. Lidin, *Angew. Chem.* **2006**, *118*, 5730 – 5734; *Angew. Chem. Int. Ed.* **2006**, *45*, 5602 – 5606; j) Z. Hugonin, M. Johnsson, S. Lidin, *Solid State Sci.* **2008**, *10*, 160 – 167; k) Z. Hugonin, M. Johnsson, S. Lidin, D. Wulferding, P. Lemmens, R. K. Kremer, *J. Solid State Chem.* **2008**, *181*, 2776 – 2782; l) R. F. Takagi, M. Johnsson, S. Lidin, *Chem. Eur. J.* **2008**, *14*, 3434 – 3441; m) D. Zhang, M. Johnsson, H. Berger, R. K. Kremer, D. Wulferding, P. Lemmens, *Inorg. Chem.* **2009**, *48*, 6599 – 6603; n) D. Zhang, H. Berger, R. K. Kremer, D. Wulferding, P. Lemmens, M. Johnsson, *Inorg. Chem.* **2010**, *49*, 9683 – 9688; o) V. Jo, M. K. Kim, D. W. Lee, I. W. Shim, K. M. Ok, *Inorg. Chem.* **2010**, *49*, 2990 – 2995; p) H. Z. Kou, Y. B. Jiang, A. L. Cui, *Cryst. Growth Des.* **2005**, *5*, 77 – 79; q) D. Zhang, M. Johnsson, R. K. Kremer, *Solid State Sci.* **2010**, *12*, 536 – 540.

[6] a) R. E. Sykora, K. M. Ok, P. S. Halasyamani, T. E. Albrecht-Schmitt, *J. Am. Chem. Soc.* **2002**, *124*, 1951 – 1957; b) R. E. Sykora, K. M. Ok, P. S. Halasyamani, D. M. Wells, T. E. Albrecht-Schmitt, *Chem. Mater.* **2002**, *14*, 2741 – 2749; c) T. C. Shehee, R. E. Sykora, M. K. Kang, P. S. Halasyamani, T. E. Albrecht-Schmitt, *Inorg. Chem.* **2003**, *42*, 457 – 462.

